ECCOMAS

Proceedia

A MULTISCALE MODELING APPROACH ON MODELING VISCO–FERROELECTRIC SELF HEATING IN FERROELECTRICS

ANDREAS WARKENTIN* AND ANDREAS RICOEUR†

*University of Kassel, Institute of Mechanics,
Moenchebergstr. 7, 34125 Kassel, Germany
e-mail: warkentin@uni-kassel.de, web page: https://www.uni-kassel.de/
e-mail: ricoeur@uni-kassel.de, web page: https://www.uni-kassel.de/

Abstract. This paper presents a hybrid microphysical/ rheological model, for describing two effects that cause a temperature change (self heating) in loaded ferroelectrics. These materials are often subjected to cyclic loading, where viscoelasticity prevails at lower electric fields, whereas dissipative heating by domain switching dominates above the coercive field. While the ferroelectric constitutive behavior is described based on a microphysical model, the viscoelasticity is modeled within a phenomenological, rheological framework. Combining both approaches leads to the hybrid model presented in this paper.

Key words: Ferroelectrics, Smart Materials, Multiphysics Problems, Self Heating, Viscoelasticity

1 INTRODUCTION

Irreversible effects in ferroelectrics, which are accompanied by energy dissipation and usually lead to an increase in temperature in the material, were previously undesirable, especially in energy harvesting, and were therefore largely avoided. The present work is based on a combination of rheological and micromechanical models, focusing on finding an appropriate thermodynamic description for capturing dissipative effects leading to temperature changes in the material. The model describes the superposition of two dissipative effects, viscoelastic and ferroelectric in nature, within a consistent theory, considering the entirety of multiphysical couplings. Simulations are based on a multiscale constitutive framework of polycrystalline ferroelectrics in connection with the so-called condensed method (CM). These theoretical considerations will further be applied to the design and optimization of cyclic processes in ferroelectric energy harvesters, exhibiting a large electrical output by exploiting the irreversible effects [1].

2   Basic equations

In addition to the nonlinear constitutive equations of a thermoelectromechanical problem

$$\sigma_{ij} = C_{ijkl}\left(\varepsilon_{kl} - \varepsilon_{kl}^{\text{irr}}\right) - e_{lij}E_l - \beta_{ij}\theta\,, \tag{1}$$

$$D_i = e_{ikl}\left(\varepsilon_{kl} - \varepsilon_{kl}^{\text{irr}}\right) + \kappa_{ij}E_j + k_i\theta + P_i^{\text{irr}}\,, \tag{2}$$

$$s = \beta_{ij}\left(\varepsilon_{ij} - \varepsilon_{ij}^{\text{irr}}\right) + k_iE_i + \gamma\theta\,, \tag{3}$$

where σ_{ij} describes the mechanical stress, D_i the electric displacement and s the specific entropy, and the electromechanical balance laws

$$\sigma_{ij,j} = 0\,, \tag{4}$$

$$D_{i,i} = 0\,, \tag{5}$$

an energy balance is required to compute the distribution of temperature change due to irreversible domain wall motions.

Furthermore, in Eq. (1) to (3) C_{ijkl}, e_{ikl}, β_{ij}, k_i, γ are the material constants of elasticity, piezoelectricity, thermal expansion, pyroelectricity and the thermal coefficient. P_i^{irr} and $\varepsilon_{kl}^{\text{irr}}$ are the irreversible polarization and irreversible strain, while the independent variables are the strain ε_{kl}, electric field E_i and temperature θ. Starting from the well known power balance resulting from rational thermodynamics and neglecting volume heat sources in relation to internal dissipation processes, the dissipative power $\dot{\chi}$ results in

$$\dot{\chi} = \dot{w}^{\text{tot}} - \dot{T}s - \dot{\phi}^{\text{free}} - \frac{T_{,i}}{T}q_i^{\text{S}} = \dot{w}^{\text{dis}} - \frac{T_{,i}}{T}q_i^{\text{S}} \geq 0\,, \tag{6}$$

where $\dot{q}_j^{\text{S}}$ is the surface heat flux, ϕ^{free} the free energy density, T the absolute thermodynamic temperature and $\dot{w}^{\text{tot}}$ and $\dot{w}^{\text{dis}}$ are the total and dissipative parts of the electromechanical power, respectively. Note, while T is the absolute thermodynamic temperature of the material

$$\theta = T - T_0 \tag{7}$$

denotes a temperature change. Additionally, to the dissipative power, from the first law of thermodynamics results the expression

$$-\dot{q}_{j,j}^S + \dot{\omega}^{\text{dis}} = T\dot{s}\,. \tag{8}$$

Inserting Eq. (3) in a rate dependent formulation in the energy balance Eq. (8) results in

$$-\dot{q}_{j,j}^S + \dot{\omega}^{\text{dis}} = T\gamma\dot{\theta}\,, \tag{9}$$

by neglecting all reversible contributions to heating or cooling in terms of the pyroelectric coefficient k_i and the contributions of the thermal stress coefficients β_{ij}. The more general integral form of Eq. (9) is

$$\int_{\Omega_2} \dot{\theta}\gamma T\,\mathrm{d}V = \int_{\Omega_1} \dot{\omega}^{\text{dis}}\,\mathrm{d}V - \int_{\partial\Omega} \dot{q}_i^{\text{S}}n_i\,\mathrm{d}A_S\,, \tag{10}$$

where Ω_1 (region of the heat source) and Ω_2 (volume around the heat source) are the considered areas and $\partial\Omega$ is the surface of Ω_2.

2.1 Transient heating with heat dissipation

In order to describe the transient heating, the heat flux $\dot{q}_\mathrm{S} = \Theta\alpha$ with $\Theta = T_\mathrm{S} - T_\infty$, α as heat transfer coefficient, T_S as the temperature on $\partial\Omega$ and T_∞ as ambient temperature, the latter assumed equal to T_0, has to be considered. Inserting the heat flux relation into Eq. (10) by using the identity $\dot{q}_i^\mathrm{S} n_i = \dot{q}_\mathrm{S}$ and assuming a homogeneous distribution of temperature change $\overline{\theta}$ in $\Omega_1 \cup \Omega_2$, the differential equation is obtained as

$$\dot{\overline{\theta}} + \frac{\alpha A_S}{T\{\gamma_i V_i\}}\overline{\theta} = \dot{\omega}^\mathrm{dis}\frac{V_{\Omega_1}}{T\{\gamma_i V_i\}} \;, \tag{11}$$

where the abbreviation

$$\sum_{i=1}^{v} \gamma_i V_i =: \{\gamma_i V_i\} \tag{12}$$

has been introduced with v as the number of all volumes with dissimilar thermal properties. A further reduction with

$$\alpha A_S/(T\{\gamma_i V_i\}) =: \tilde{\kappa} \tag{13}$$

and

$$V_{\Omega_1}/(T\{\gamma_i V_i\}) =: \tilde{\beta} \tag{14}$$

provides

$$\dot{\overline{\theta}} + \tilde{\kappa}\overline{\theta} = \tilde{\beta}\dot{\omega}^\mathrm{dis} \;. \tag{15}$$

The solution of this differential equation in terms of to $\overline{\theta}$, using Eq. (7), is obtained as follows:

$$\overline{\theta}(t) = \dot{\omega}^\mathrm{dis} f^\mathrm{g}(t) = \dot{\omega}^\mathrm{dis}\frac{V_{\Omega_1}}{\alpha A_S}\left(1 - \mathrm{e}^{-\tilde{\kappa}t}\right) \;, \tag{16}$$

where $f^\mathrm{g}(t)$ is a geometry– and time–dependent function, not depending on the calculations from the CM [2]. Rewriting the solution of the differential equation within the context of the CM provides the macroscopic multi–grain formulation

$$\overline{\theta}(t) = \langle\dot{\omega}^\mathrm{dis}\rangle f^\mathrm{g}(t) = \langle\dot{\omega}^\mathrm{dis}\rangle\frac{V_{\Omega_1}}{\alpha A_S}\left(1 - \mathrm{e}^{-\tilde{\kappa}t}\right) \;, \tag{17}$$

where angled brackets denote quantities averaged over $M \in \mathbb{N}$ grains of a representative volume element (RVE), i.e.

$$\langle\xi\rangle := \frac{1}{M}\sum_{m=1}^{M}\xi^m \;, \; \forall m \in \{1, ..., M\} \tag{18}$$

and bars denote homogeneous quantities in the context of a generalized VOIGT approximation. Of course, a model for describing the dissipation power is needed. Thus, in the next section, a model for describing the material behavior of ferroelectrics is discussed.

3 Hybrid micromechanical–rheological modeling

A hybrid micromechanical–rheological model is developed as depicted in Fig. 1. Each grain of the material is represented by at least one classical rheological model modified by a component which represents the microstructure of the domains resulting from a micromechanical model, Fig. 2. The micromechanical model initially was developed by Huber et al. [4]. In order
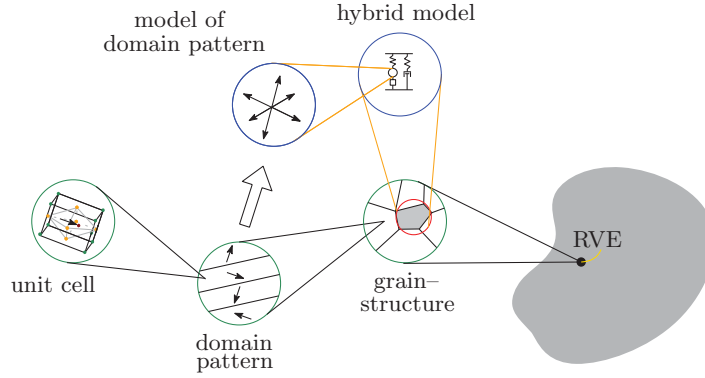

Figure 1: Hybrid micromechanical–rheological model, representing a grain of an RVE, consisting of a classical rheological model containing an additional component representing the microstructure which results from the microphysical model, see [3].

to map the domain pattern of a grain with $N \in \mathbb{N}$ possible directions of spontaneous polarization, indicated by the arrows in Fig. 2, internal variables $\nu^{(n)} \in [\nu^{\min}, 1]$ with $n \in \{1, ..., N\}$ and $\nu^{\min} \geq 0$ are introduced. Furthermore, the internal variables have to fulfill the partition of unity

$$\sum_{n}^{N} \nu^{(n)} = 1 \,. \tag{19}$$

Here, the internal variable $\nu^{(n)}$ weight the volume fraction of the domain n, e.g., in the unpolarized state, the condition $\nu^{(n)} = N^{-1}$ holds, meaning that the volume fractions of all domains are identical. Hwang et al. (1995) proposed an energy–based switching criterion [6]

$$\omega_{(n)}^{\mathrm{diss}} \geq \omega_{\mathrm{crit}}^{(\beta)} \,, \tag{20}$$

stating that switching only occurs, if the associated dissipative energy of a domain $\omega_{\mathrm{diss}}^{(n)}$ is larger than a critical value, depending on the switching angle β. Furthermore, rational thermodynamics provides a relation between the dissipative work rate of a domain and the internal variables:

$$\dot{\omega}^{\mathrm{dis}} = -\sum_{n=1}^{N} \frac{\partial \phi^{\mathrm{free}}}{\partial \nu^{(n)}} \dot{\nu}^{(n)} \,. \tag{21}$$
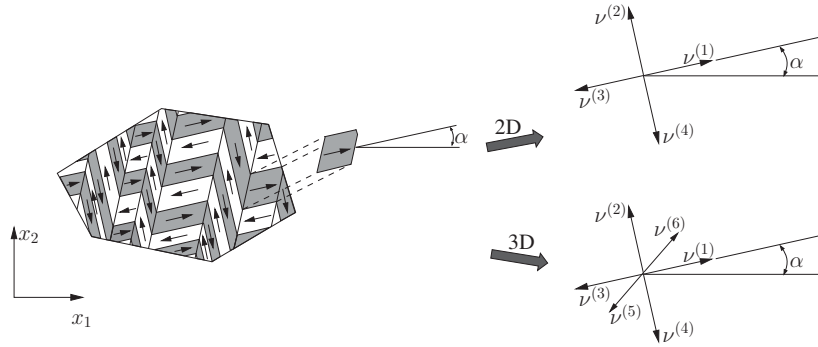
Figure 2: Two dimensional depiction of a tetragonal domain structure of a grain (left) with orientation a in global coordinate system (x_1, x_2) and representation by internal variables $\nu^{(n)}$ in 2D and 3D models. see [5].

Thus, the dissipation power according to Eq. (6) results in

$$\dot{\chi} = -\sum_{n=1}^{N} \frac{\partial \phi^{\text{free}}}{\partial \nu^{(n)}} \dot{\nu}^{(n)} - \frac{1}{T} T_{,i} q_i^{\text{S}} \geq 0 \,. \tag{22}$$

Obviously, changes in domain volume fractions lead to dissipation. The changes of volume fractions are expressed by an evolution equation, see [7].

In order to obtain a mathematical framework of the hybrid model, depicted in Fig. 1, a more detailed illustration is given in Fig 3. Following the classical procedure concerning rheological
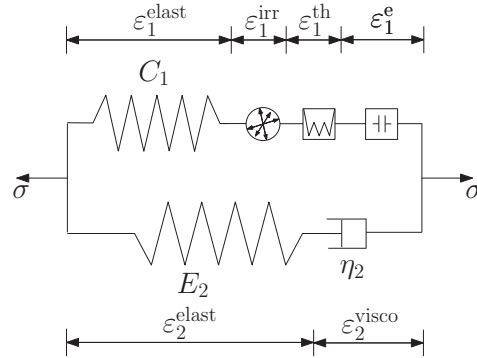

Figure 3: Hybrid micromechanical–rheological model and the explicit partition of the strain fractions of the respective components, see [3]

models, both the relations for total strain

$$\begin{aligned} \varepsilon^{\text{tot}} &= \varepsilon_1^{\text{elast}} + \varepsilon_1^{\text{th}} + \varepsilon_1^{\text{e}} + \varepsilon_1^{\text{irr}} \\ &= \varepsilon_2^{\text{elast}} + \varepsilon_2^{\text{visco}} \end{aligned} \tag{23}$$

with elastic $\varepsilon_1^{\text{elast}}$, thermal $\varepsilon_1^{\text{th}}$, electrical ε_1^{e}, irreversible $\varepsilon_1^{\text{irr}}$ and viscoelastic $\varepsilon_2^{\text{visco}}$ strain components, and the constitutive equation of the stresses

$$
\begin{aligned}
\sigma = \sigma_1^{\text{eq}} + \sigma_2^{\text{ov}} &= C_1 \varepsilon_1^{\text{elast}} + E_2 \varepsilon_2^{\text{elast}} \\
&= C_1 \{ \varepsilon^{\text{tot}} - \varepsilon_1^{\text{th}} - \varepsilon_1^{\text{e}} - \varepsilon_1^{\text{irr}} \} \\
&\quad + E_2 \{ \varepsilon^{\text{tot}} - \varepsilon_2^{\text{visco}} \}
\end{aligned}
\tag{24}
$$

are involved, whereupon just one–dimensional formulation are given in Eqs. (23) to (24) for the sake of simplicity. C_1 and E_2 represent the stiffness of the springs. Furthermore, an evolution equation for the viscous strain rate as further internal variable is introduced according to

$$
\dot{\varepsilon}_2^{\text{visco}} = \frac{\sigma_2^{\text{ov}}}{\eta_2} = \frac{E_2}{\eta_2} \{ \varepsilon^{\text{tot}} - \varepsilon_2^{\text{visco}} \} ,
\tag{25}
$$

where σ_2^{ov} is the over stress describing the stress in the branch where the damper is placed. In the case of the hybrid model, rational thermodynamics provides a relation between the dissipative work rate of a domain species of a grain and both types of internal variables assembled in $\{q\}$:

$$
\dot{\omega}^{\text{dis}} = \dot{\omega}_{(\text{ferro})}^{\text{dis}} + \dot{\omega}_{(\text{visco})}^{\text{dis}} = -\frac{\partial \phi^{\text{free}}}{\partial \{q\}} \{ \dot{q} \} = -\sum_{n=1}^{N} \frac{\partial \phi^{\text{free}}}{\partial \nu^{(n)}} \dot{\nu}^{(n)} - \frac{\partial \phi^{\text{free}}}{\partial \varepsilon_2^{\text{visco}}} \dot{\varepsilon}_2^{\text{visco}}
\tag{26}
$$

Furthermore, the dissipation power of the hybrid model reads

$$
\dot{\chi} = -\frac{\partial \phi^{\text{free}}}{\partial \{q\}} \{ \dot{q} \} - \frac{1}{T} T_{,i} q_i^{\text{S}} \geq 0 .
\tag{27}
$$

The work rate regarding viscoelasticity is given by following the classical scheme for describing rheological models:

$$
\dot{\omega}_{(\text{visco})}^{\text{dis}} = \frac{1}{\eta} \sigma_{ij}^{\text{ov}} \dot{\varepsilon}_{ij}^{\text{visco}} .
\tag{28}
$$

The dissipative work rate regarding ferroelectricity is described e.g. in [2] as

$$
\dot{\omega}_{(\text{ferro})}^{\text{dis}} = \sigma_{ij}^{\text{eq}} \dot{\varepsilon}_{ij}^{\text{irr}} + E_i \dot{P}_i^{\text{irr}} .
\tag{29}
$$

4   Results

This section shows results of a numerical simulation for the investigation of temperature development in polycrystalline PZT ferroelectrics, compared to an experimental result in [8].

Fig. 4(a) shows the loading scheme for the numerical example, and Fig. 4(b) shows the corresponding temperature change of the PZT. Starting from Eqs. (17), (26), (28) and (29), holding in the style of the CM, see Eq. (18), Fig. 4(b) shows the numerical results for the temperature development compared to the experimental result from [8]. The thermal coefficients in f^{g}

from Eq. (17) are obtained by using the thermal characteristic time which is identified from the experimental measured temperature curve from [8].
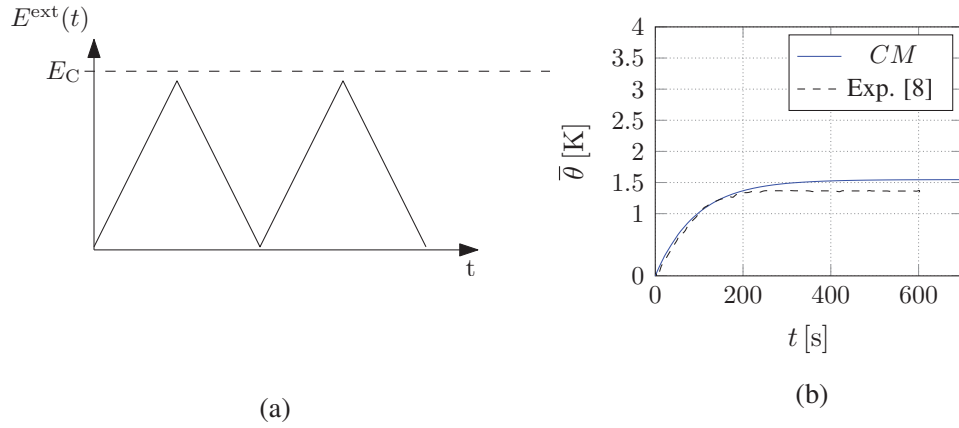

(a)

(b)

Figure 4: Comparison of the temperature $\overline{\theta}$ vs. time t at a frequency $f=100$ Hz of the unipolar external electrical load resulting from simulation (CM) and experiment from [3]; blue line: simulation results from the CM for a polycrystalline material, black line: experimental results from [8]

For the simulation, a polycrystal with 60 grains in a RVE is employed and a unipolar electric load $E^{\text{ext}} = 0.8\, E_{\text{C}}$ in the style of Fig. 4(a) is applied, where E_{C} is the coercivity of the material. Due to the fact, that the external electric field does not reach the value of the coercive field, no damain–wall motion takes place, the heating is only due to viscoelasticity. Furthermore, a constant dissipation rate is assumed. Nevertheless, the result from the simulation, solid blue line, is in good agreement with the experimental result [8].

5 Conclusions

Generally, both viscoelasticity and domain switching lead to dissipative heating in ferro-electrics, the latter effect dominating above the coercive field and typically amounting to 10–15 K [9]. With the presented new hybrid micromechanical–rheological model, obviously it is possible to calculate correctly the temperature from self–heating due to viscoelastic effects, see Fig. 4. Viscoelasticity contributes, as shown with 1.4 K at 100 Hz.

REFERENCES

[1] L. Behlen, A. Warkentin, and A. Ricoeur, "Exploiting ferroelectric and ferroelastic effects in piezoelectric energy harvesting: Theoretical studies and parameter optimization," *Smart Materials and Structures*, vol. 30, no. 3, p. 035031, Feb. 2021.

[2] S. Lange and A. Ricoeur, "A condensed microelectromechanical approach for modeling

tetragonal ferroelectrics," *International Journal of Solids and Structures*, vol. 54, pp. 100–110, Feb. 2015.

[3] A. Warkentin and A. Ricoeur, "Hybrid modeling of viscoelastic and switching–induced heating in ferroelectrics," *PAMM*, vol. 22, no. 1, Mar. 2023.

[4] J. Huber, "A constitutive model for ferroelectric polycrystals," *Journal of the Mechanics and Physics of Solids*, vol. 47, no. 8, pp. 1663–1697, Aug. 1999.

[5] A. Warkentin and A. Ricoeur, "A semi-analytical scale bridging approach towards polycrystalline ferroelectrics with mutual nonlinear caloric-electromechanical couplings," *International Journal of Solids and Structures*, vol. 200–201, pp. 286–296, Sep. 2020.

[6] S. C. Hwang, C. S. Lynch, and R. M. McMeeking, "Ferroelectric/ferroelastic interactions and a polarization switching model," *Acta Metallurgica et Materialia*, vol. 43, no. 5, pp. 2073–2084, May 1995.

[7] A. Ricoeur and S. Lange, "Constitutive modeling of polycrystalline multiconstituent and multiphase ferroic materials based on a condensed approach," *Archive of Applied Mechanics*, Jan. 2019.

[8] M. S. Senousy, R. K. N. D. Rajapakse, D. Mumford, and M. S. Gadala, "Self-heat generation in piezoelectric stack actuators used in fuel injectors," *Smart Materials and Structures*, vol. 18, no. 4, p. 045008, Apr. 2009.

[9] A. Warkentin and A. Ricoeur, "Experimental investigations of viscoelastic and ferroelectric heating in PZT–5H," in *PAMM*, vol. 20, 2020, p. e202000198.